Available online at www.sciencedirect.com

SciVerse ScienceDirect

journal homepage: www.elsevier.com/locate/he

Nanoconfined mixed Li and Mg borohydrides as materials for solid state hydrogen storage

Giovanni Capurso [a,*], Filippo Agresti [b], Laura Crociani [c], Gilberto Rossetto [c], Benedetto Schiavo [d], Amedeo Maddalena [a], Sergio Lo Russo [e], Giovanni Principi [a]

[a] Dipartimento di Ingegneria Industriale, Università di Padova, via Marzolo 9, 35131 Padova, Italy
[b] Istituto per l'Energetica e le Interfasi, CNR Padova, Italy
[c] Istituto di Chimica Inorganica e delle Superfici, CNR Padova, Italy
[d] Dipartimento di Fisica, Università di Palermo, and Istituto per le Tecnologie Avanzate, Trapani, Italy
[e] Dipartimento di Fisica e di Astronomia "Galileo Galilei" and CNISM, Università di Padova, Italy

ARTICLE INFO

Article history:
Received 10 February 2012
Received in revised form
20 April 2012
Accepted 21 April 2012
Available online 17 May 2012

Keywords:
Hydrogen storage
Lithium borohydride
Magnesium borohydride
Nanoconfinement

ABSTRACT

Several mixtures of $LiBH_4$ and $Mg(BH_4)_2$ borohydrides in different stoichiometric ratios (1:0, 2:1, 1:1, 1:2, 0:1), prepared by high energy ball milling, have been investigated with X-ray powder diffraction and thermal programmed desorption (TPD) volumetric analysis to test the dehydrogenation kinetics in correlation with the physical mixture composition. Afterwards mixed and unmixed borohydrides were dispersed on high specific surface area ball milled graphite by means of the solvent infiltration technique. BET and statistical thickness methods were used to characterize the support surface properties, and SEM micrographs gave a better understanding of the preparation techniques. It has been observed by TPD volumetric measurements that the confinement of the reactive borohydrides on the nanoporous supports leads to a lower dehydrogenation temperature compared to unsupported borohydrides. Moreover, a further decrease of the dehydrogenation temperature has been observed by increasing the specific surface area of the support and the pores volume and by using the prepared mixtures instead of pure materials. The dehydrogenation process seems to be favoured by the heterogeneous nucleation on the graphite surface of decomposition products or intermediate phases from melted liquid borohydrides.

1. Introduction

One essential component for successful clean power technologies is hydrogen storage in a convenient way for on-board and stationary applications. At present, targets for reversible hydrogen storage materials require characteristics that will finally give a gravimetric capacity of 5.5 wt% hydrogen to storage devices [1]. Because it is not likely that capacities higher than 6 wt% can be obtained in transition metal hydride materials, research and studies have focused on complex hydrides of few light elements, for instance alanates, amides and borohydrides.

Light alkaline and alkaline-earth metal based borohydrides, as $LiBH_4$ and $Mg(BH_4)_2$, are interesting materials as potential hydrogen storage media, owing to their high theoretical hydrogen storage capacities [2,3]. The most commonly

* Corresponding author. Tel.: +39 (0) 49 827 5828; fax: +39 (0) 49 827 5505.
E-mail address: giovanni.capurso@gmail.com (G. Capurso).
0360-3199/$ – see front matter
doi:10.1016/j.ijhydene.2012.04.111

suggested decomposition pathways [4,5] lead to high gravimetric capacities:

$$LiBH_4 \rightarrow LiH + B + 3/2H_2 \quad 13.9\ wt\% \tag{1}$$

$$Mg(BH_4)_2 \rightarrow MgB_2 + 4H_2 \quad 14.9\ wt\%, \tag{2}$$

but with several limitations of the hydrogen exchanging thermodynamics and kinetics, which also hinder the reversible dehydrogenation. In order to overcome these limitations, it has been proposed to confine the hydrides in nanoporous scaffolds, exploiting the favourable properties of nanostructured materials which can be employed to tailor the size, surface and morphology features of hydride reactants [6], besides to avoid sintering and agglomeration during cycling. It has been shown that $LiBH_4$ milled or combined with carbon nanotubes [7,8] and included in mesoporous carbon [9] displays a decrease of the dehydrogenation temperature.

The thermodynamic properties of a storage material can be also controlled getting chemical stability of the dehydrogenated state, thus diminishing the enthalpy for dehydrogenation [10].

Destabilization of complex hydrides with reactive systems allows to increase dramatically the performances of individual materials [6,11].

Beneficial effects of carbon addition on the dehydrogenation kinetics have also been observed for the Li–B–Mg–H system [12].

This paper is an attempt to show the synergistic effects of the two mentioned destabilization methods: it is shown that ball milled mixtures of $LiBH_4$ and $Mg(BH_4)_2$ deposited on graphite exhibit a lower onset dehydrogenation temperature compared to supported individual materials or unsupported reactive mixtures.

2. Experimental

The lithium borohydride powder was purchased from Sigma–Aldrich (>95% pureness) and the magnesium borohydride was synthesized from $MgBut_2$ and BH_3SMe_2 [13] following the method described in [14].

Mixtures of these two products, $LiBH_4$:$Mg(BH_4)_2$ with stoichiometric ratios 1:0, 2:1, 1:1, 1:2, 0:1 were obtained by ball milling in Ar atmosphere for 15 h using a SPEX 8000M shaker mill with a ball to powder ratio of 10:1 in a hardened steel vial with stainless steel spheres. The masses of the starting materials used for a typical throughput of 1 g are reported in Table 1. Samples A and E are the initial materials after ball milling.

Table 1 – Masses used for ball-milling of unmixed and mixed borohydrides, with a throughput of 1 g.

Sample and stoichiometry	$LiBH_4$ (g)	$Mg(BH_4)_2$ (g)
A (1:0)	1.000	0.000
B (2:1)	0.449	0.551
C (1:1)	0.289	0.711
D (1:2)	0.169	0.831
E (0:1)	0.000	1.000

Smaller amounts of pure and mixed samples, typically a tenth of gram, were soluted in 50 ml of methyl tert-butyl ether (MTBE) (Sigma–Aldrich, anhydrous, 99.8%) and stirred for 24 h in protective atmosphere vials.

Microporous graphite, starting from commercial graphite purchased from Carlo Erba Reagenti was obtained by milling it in the conditions reported before for different times: 15, 90 and 600 minutes (in this last case 660 min adding 10 min pause every hour). Its characterization was done with N_2 adsorption measurements at 77 K using a Quantachrome Nova 1200e Surface Area and Pore Analyzer. Specific surface areas (SSA) of the different supports were calculated by means of multipoint Brunauer–Emmet–Teller (BET) method (in the range $0.02–0.3p/p_0$), while the micropore area was derived with de Boer statistical thickness method in the range from 0.2 to $0.5p/p_0$.

The milled graphite was degassed at 300 °C in rotary vacuum and then poured into the solution of borohydride mixtures in MTBE and stirred for further 24 h. Afterwards it was dried using a Schlenk flask connected to rotary pump vacuum and, finally, heated to 100 °C for 3 h.

Thermal programmed desorption (TPD) measurements were performed on the produced samples by means of a calibrated Sievert's volumetric apparatus supplied by Advanced Materials Corporation.

X-ray diffraction (XRD) patterns of milled samples were obtained using a Bruker D8 Advance diffractometer with Bragg–Brentano geometry and Cu Kα radiation. The samples were protected with a thin kapton foil (8 μm).

Scanning electron microscopy (SEM) micrographs were acquired with a JEOL JSM-6490 scanning electron microscope operated at 20 kV.

Differential scanning calorimetry (DSC) measurements were performed using a DSC-1 (Mettler Toledo) instrument. The samples were charged inside 40 μl aluminium pans, which were sealed by cold welding, using a suitable press. The temperature and enthalpy calibrations for the DSC instrument were checked by measuring melting temperature and enthalpy of tin and indium standards [15].

All samples and carbonaceous supports were handled into an M-Braun glove box equipped with a gas purification system (less than 0.1 ppm water and 1 ppm O_2).

3. Results and discussion

3.1. *Borohydride mixtures*

The XRD patterns shown in Fig. 1 belong to the as milled mixtures of borohydrides at different ratios. Samples A and E display the diffraction peaks of the low temperature stable phases for starting borohydrides: in the pattern of sample A all the peaks for orthorhombic phase of $LiBH_4$ are labelled and the pattern of sample E is almost completely attributable to α-$Mg(BH_4)_2$ phase with minor contribution of β-$Mg(BH_4)_2$ phase. In all milled samples a small loss of cristallinity can be noticed with respect to the as-received or as-synthesized products, causing little broadening, shift and differences in the intensity ratios of peaks. To improve the diffraction patterns and the characterization of the samples a mild annealing treatment

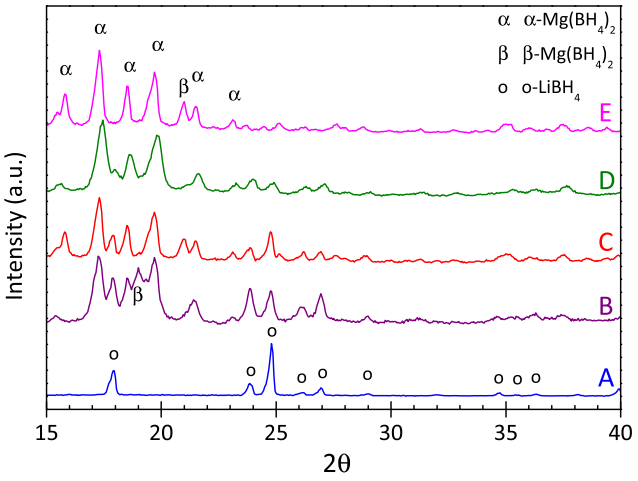

Fig. 1 – XRD patterns of ball milled borohydrides and borohydride mixtures (labelled as in Table 1).

has been tried, heating the samples at 150 °C in H_2 atmosphere for 6 h. The patterns obtained after this treatment added no further information to those shown in Fig. 1, so they are not reported.

The XRD patterns of the mixed borohydrides can be described as a combination of the already identified stable phases: going from B to D there is an increasing contribution of α-$Mg(BH_4)_2$ and an obvious decrease of $LiBH_4$ peaks. There is no evidence of any dual-cation borohydride formation in the process of milling, as proposed by Fang et al. [16] and already confuted by Bardají et al. [17].

In Fig. 2 the TPD analysis profiles performed on the 5 different samples are reported: lines A and E represent pure $LiBH_4$ and pure $Mg(BH_4)_2$, respectively, while the other lines refer to mixed samples, which give intermediate properties between the pure borohydrides, as for the XRD pattern behaviour.

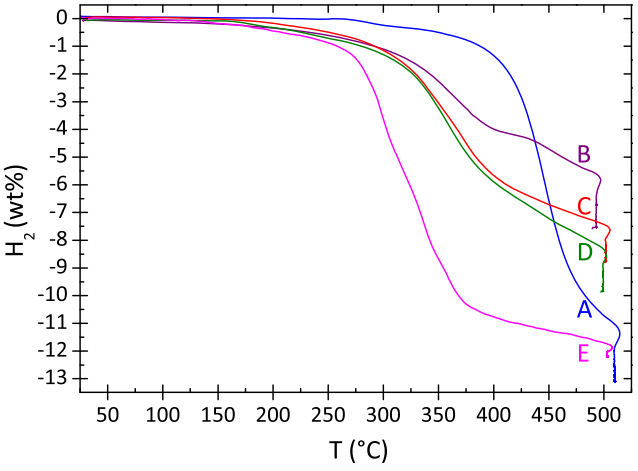

Fig. 2 – Thermal programmed desorption profiles of milled borohydrides and physical borohydride mixtures (see Table 1 for labels) at a heating rate of 2.5 °C/min and starting in vacuum.

All the mixed samples perform the desorption process between the two pure materials, so in this case it is not possible to notice the improvement claimed in similar works [16–18] and, moreover, the final amount of released hydrogen is lower than expected. Presumably, the milling process carried out here with a shaker mill, more energetic than the planetary mills used in [16–18], produced a slight contamination or caking of powders due to increase of local temperature. We argue that a too energetic milling is not effective to create a mixture where the polymorphic transformations are assisted by the presence of the second component.

3.2. *Support characterization*

The results of morphological characterization of the milled graphite to be used as support of the borohydrides are reported in Table 2 and Fig. 3.

The results of BET and micropore analysis are summarized in Table 2. The values of SSA are increasing with longer milling time, due to the presence of micropores, but the external surface area, in particular from sample III to IV, is not following this trend. The cause can be better understood observing the SEM pictures of Fig. 3. It is clearly visible how the pristine structure of the as received graphite is still visible after milling by 15 min, but destroyed after 90 min and especially after 10 h, when the lamellar particles are completely replaced by a disordered powder with rough and eventually porous surface.

3.3. *Impregnated samples*

The TPD curves in Fig. 4 represent a clear evidence of lowering the hydrogen release temperature when a hydride is impregnated into a high SSA material. Impregnated samples are labelled X_Y, where X is the milled samples (Table 1) and Y is the support used (Table 2). The higher the SSA, the stronger is this effect: the temperature for the main release (when most of the H_2 is released at the fastest rate) is shifted by almost 100 °C in the sample A_{IV} if compared with A (not impregnated $LiBH_4$). Of course, the use of milled graphite is decreasing the storage gravimetric capacity; with A_I, the use of as received graphite seems to have even a detrimental effect in the temperature, but this is due to the lower released amount that stretches the curve with respect to A_0.

It is possible to conclude that the as received graphite is having almost no effect on release temperature, due to the low specific surface area. This is better comprehensible looking at the derivative of the desorption profiles, that give a qualitative representation of the hydrogen flow and confirm what stated before.

Table 2 – SSA analysis of graphite after ball milling.

Graphite (BM time)		External SSA (m^2/g)	Micropores (m^2/g)
I	(as received)	9	0
II	(15 min)	55	7
III	(90 min)	256	73
IV	(10 h)	182	115

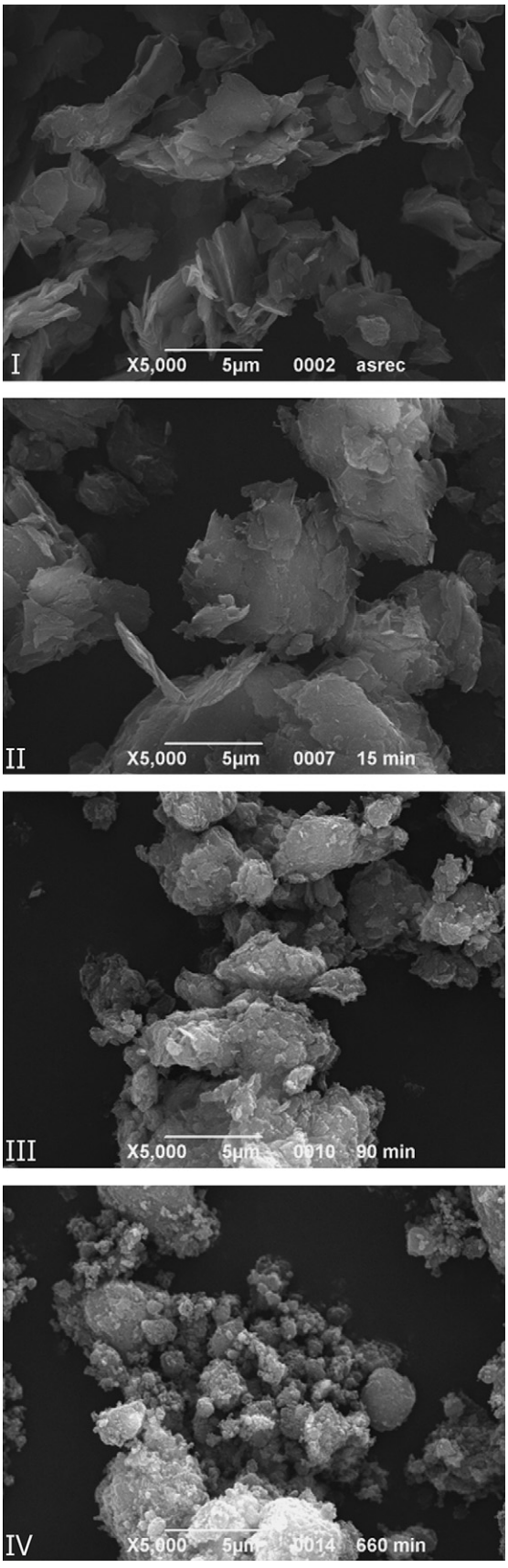

Fig. 3 – SEM pictures for graphite at different milling times (see Table 2).

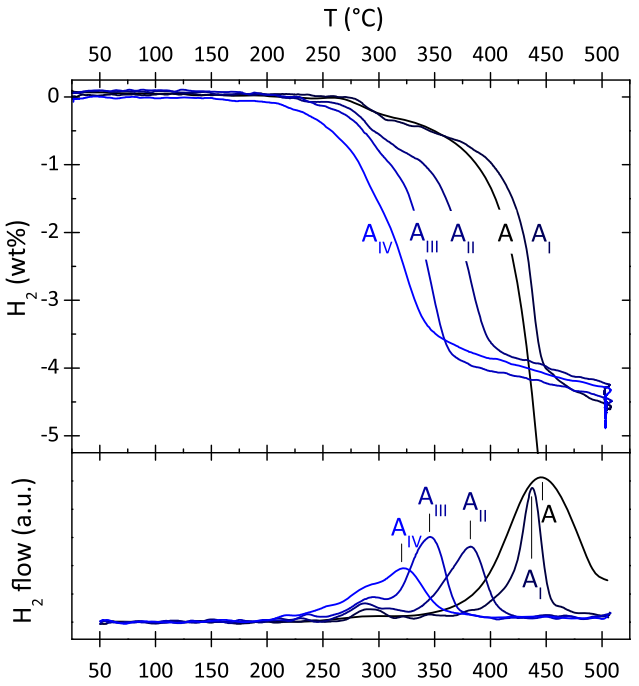

Fig. 4 – Thermal programmed desorption curves (top) and corresponding derivative (bottom) for sample A (see Table 1) on different SSA graphite supports (see Table 2), at a heating rate of 2.5 °C/min and starting in vacuum.

On the basis of the results shown in Fig. 4, the 10 h milled graphite (IV) was chosen as the most convenient scaffold for impregnation of mixed and unmixed borohydrides.

Fig. 5 shows the results of XRD analysis of these samples, as well as the pattern of milled graphite IV. The effect of confinement is clearly evident in all samples, particularly in those containing a higher percentage of $Mg(BH_4)_2$. Starting from pattern A_{IV}, where all the peaks for $LiBH_4$ are broad, moving to higher magnesium borohydride content, a slight increase in the intensity of background profile (centred at

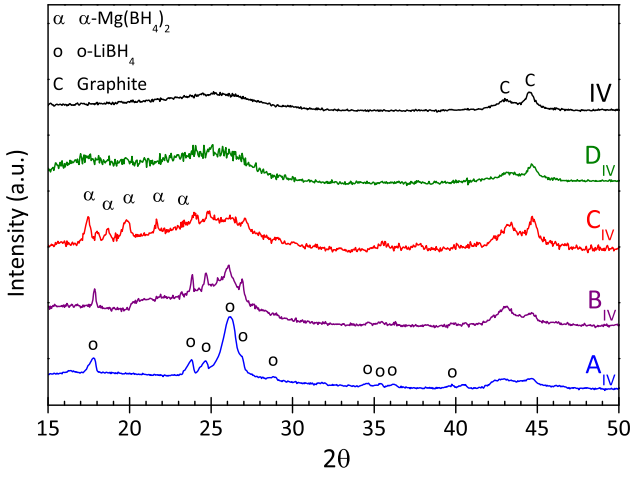

Fig. 5 – XRD patterns of samples A_{IV}, B_{IV}, C_{IV}, D_{IV}, after impregnation in the milled graphite, represented by pattern IV (see Tables 1 and 2).

about $2\theta = 25°$) can be observed. In pattern B_{IV} it is hard to detect traces of α-$Mg(BH_4)_2$, which become more visible in C_{IV} and then disappear in pattern D_{IV}, where are replaced by a second hump at lower angles. Pattern of sample E_{IV} (not shown) is similar to this last one, where no phases were detectable besides graphite. A plausible reason for this behaviour is that α-$Mg(BH_4)_2$ is more prone to nucleate as small particles or amorphous material inside the graphite.

The TPD analysis on dispersed borohydrides is shown in Fig. 6. Starting from sample A_{IV} (i.e. the same shown in Fig. 4), the desorption temperature is lowered of further tens of degrees. Sample E_{IV} (pure supported $Mg(BH_4)_2$) displays a TPD profile starting after 200 °C with a maximum of flow at 275 °C, while the samples B_{IV} and D_{IV} present a broad flow profile with a maximum around 300 °C: the shape indicates that desorption starts at a lower temperature and occurs in a wide interval of time. The best behaviour in terms of lowering the temperature is that of sample C_{IV}, the flow peak of which is at about 260 °C.

All the samples have a gravimetric capacity between 3 and 4 wt%, except for A_{IV}, which is one point higher.

In Fig. 7, the DSC profiles in the range 30–240 °C of samples simply mixed in a mortar are reported. It is possible to observe the endothermic polymorphic transformation of $LiBH_4$ at approximately 113 °C and a second two peaks endothermic event at about 180 °C. The first is probably generated by the shifting of the $Mg(BH_4)_2$ phase transformation, as suggested in [17]. The other peak corresponds to the melting of the mixture. This low melting temperature is supposed to be one of the causes of the lower decomposition temperature of the studied borohydride mixture when this is nanoconfined on high SSA

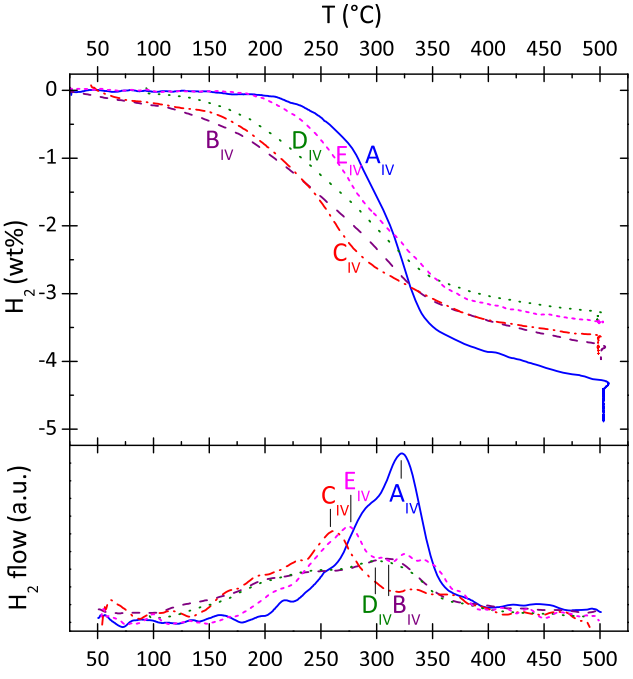

Fig. 6 – Thermal programmed desorption curves (top) and corresponding derivative (bottom) for base materials and mixed samples on milled graphite IV (see Tables 1 and 2) at a heating rate of 2.5 °C/min and starting in vacuum.

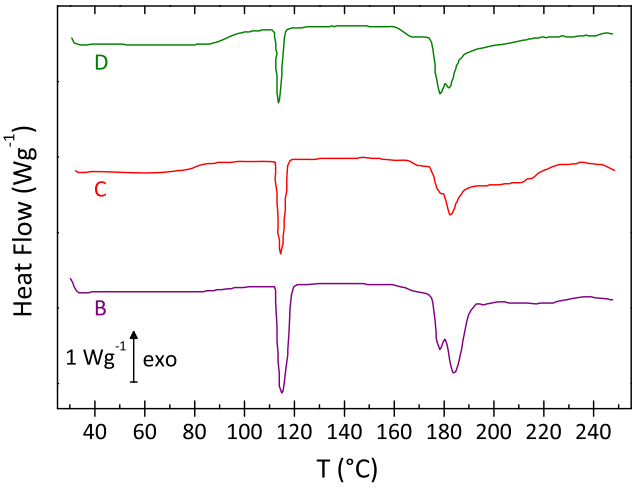

Fig. 7 – DSC profiles of the mixed samples (see Table 1 for stoichiometry), with a heating ramp of 5 °C/min in 80 ml/min Ar flow.

supports: heterogeneous nucleation of decomposition products can occur from melted borohydride. The tentative phase diagram reported in [17] is showing, in fact, that a possible eutectic point is situated close to the 1:1 stoichiometry of sample C_{IV}, which is the one with lower desorption temperature. The decomposition is also probably favoured by the presence of sites where the nuclei with the same critical radius and a smaller volume can overcome the nucleation energy gap. So, raising the surface available for heterogeneous nucleation (the SSA of the support), and having a favourable morphology, it is possible to improve the reaction kinetics [8]. To further support this hypothesis, single point BET surface area measurements carried out on nanoconfined samples gave values one order of magnitude lower than those measured on the as milled graphite (about 8 m^2/g in comparison with values in Table 2). This can suggest that the active material, the mixed borohydride, was effectively dispersed on the available surface filling the micropores. Further investigations are in progress to clarify this point.

Interestingly, nanoconfinement of hydrides has been suggested as a way to control the released gases, limiting undesired desorptions [19]. Experiments are in progress also in this direction.

4. Conclusions

In order to investigate the effect of confinement in the nanoporous supports on mixed borohydride systems, composites of $LiBH_4$ and $Mg(BH_4)_2$ borohydrides in five different ratios have been prepared by ball milling and dispersed on a high SSA graphite.

While TPD analysis of the physical mixture has not shown improvements in this case, it has been observed by volumetric measurements that the confinement lowers the dehydrogenation temperature with respect to not confined samples. There is a link between the available surface and pores area of

the support and the release temperature of the system: it has been found that the support used in this investigation decreased the dehydrogenation temperature with respect to the pure material by more than 100 °C. The process appears to be facilitated by the nucleation of decomposition products or intermediate phases from melted borohydrides on the graphite surface and pores.

Acknowledgements

GC is grateful to Dr. Ashish Khandelwal for organized data and files. Work funded partly by the Progetto di Ateneo 2010 entitled "Innovative methods for solid state hydrogen storage: dispersion of hydrides on supports with high SSA" and partly by the project "HYDROSTORE" in the frame of the Industria 2015 Program, call Energy Efficiency.

REFERENCES

[1] "DOE targets for onboard hydrogen storage systems for light-duty vehicles", September 2009, retrieved from: http://www1.eere.energy.gov/hydrogenandfuelcells/storage/pdfs/targets_onboard_hydro_storage.pdf [on 30.06.11].
[2] Sakintuna B, Lamari-Darkrim F, Hirscher M. Metal hydride materials for solid state hydrogen storage. Int J Hydrogen Energy 2007;32:1121–40.
[3] Orimo S, Nakamori Y, Eliseo JR, Züttel A, Jensen CM. Complex hydrides for hydrogen storage. Chem Rev 2007;107:4111–32.
[4] Züttel A, Rentsch S, Fischer P, Wenger P, Sudan P, Mauron P, et al. Hydrogen storage properties of $LiBH_4$. J Alloys Compd 2003;356-357:515–20.
[5] Chłopek K, Frommen C, Léon A, Zabara O, Fichtner M. Synthesis and properties of magnesium tetrahydroborate, $Mg(BH_4)_2$. J Mater Chem 2007;17:3496–503.
[6] Vajo JJ, Olson GL. Hydrogen storage in destabilized chemical systems. Scr Mater 2007;56:829–34.
[7] Yu XB, Wu Z, Chen QR, Li ZL, Weng BC, Huang TS. Improved hydrogen storage properties of $LiBH_4$ destabilized by carbon. Appl Phys Lett 2007;91:034106.
[8] Agresti F, Khandelwal A, Capurso G, Lo Russo S, Maddalena A, Principi G. Improvement of dehydrogenation kinetics of $LiBH_4$ dispersed on modified multi-walled carbon nanotubes. Nanotechnology 2010;21:065707.
[9] Cahen S, Eymery JB, Janot R, Tarascon JM. Improvement of the $LiBH_4$ hydrogen desorption by inclusion in mesoporous carbon. J Power Sources 2009;189:902–8.
[10] Vajo JJ, Skeith SL. Reversible storage of hydrogen in destabilized $LiBH_4$. J Phys Chem B 2005;109:3719–22.
[11] Crosby K, Shaw LL. Dehydriding and re-hydriding properties of high-energy ball milled $LiBH_4 + MgH_2$ mixtures. Int J Hydrogen Energy 2010;35:7519–29.
[12] Wang PJ, Fang ZZ, Ma LP, Kang XD, Wang P. Effect of carbon addition on hydrogen storage behaviors of Li–Mg–B–H system. Int J Hydrogen Energy 2009;35:3072–5.
[13] Zanella P, Crociani L, Masciocchi N, Giunchi G. Facile high-yield synthesis of pure, crystalline $Mg(BH_4)_2$. Inorg Chem 2007;46:9039–41.
[14] Zanella P, Crociani L, Giunchi G. Process for the preparation of crystalline magnesium borohydride. U.S. patent; 2007/0286787.
[15] Grønvold F. Enthalpy of fusion and temperature of fusion of indium, and redetermination of the enthalpy of fusion of tin. J Chem Thermodynamics 1993;25:1133–44.
[16] Fang ZZ, Kang XD, Wang PJ, Li HW, Orimo SL. Unexpected dehydrogenation behavior of $LiBH_4/Mg(BH_4)_2$ mixture associated with the in situ formation of dual-cation borohydride. J Alloys Compd 2010;491:L1–4.
[17] Bardají EG, Zhao-Karger Z, Boucharat N, Nale A, van Setten MJ, Lohstroh W, et al. $LiBH_4$–$Mg(BH_4)_2$: a physical mixture of metal borohydrides as hydrogen storage material. J Phys Chem C 2011;115:6095–101.
[18] Nale A, Catti M, Bardají EG, Fichtner M. On the decomposition of the $0.6LiBH_4 - 0.4Mg(BH_4)_2$ eutectic mixture for hydrogen storage. Int J Hydrogen Energy 2011;36:13676–82.
[19] Liu X, Peaslee D, Jost CZ, Baumann TF, Majzoub EH. Systematic pore-size effects of nanoconfinement of $LiBH_4$: elimination of diborane release and tunable behavior for hydrogen storage applications. Chem Mater 2011;23:1331–6.